

Received June 9, 2018, accepted July 7, 2018, date of publication July 23, 2018, date of current version October 8, 2018.

Digital Object Identifier 10.1109/ACCESS.2018.2858856

Remaining Useful Life Prediction for Lithium-Ion Battery: A Deep Learning Approach

LEI REN^{1,2}, (Member, IEEE), LI ZHAO¹, SHENG HONG^{1,3}, SHIQIANG ZHAO¹,
HAO WANG^{1,4}, (Member, IEEE), AND LIN ZHANG^{1,2}, (Senior Member, IEEE)

¹School of Automation Science and Electrical Engineering, Beihang University, Beijing 100191, China

²Engineering Research Center of Complex Product Advanced Manufacturing System, Ministry of Education, Beijing 100191, China

³School of Cyber Science and Technology, Beihang University, Beijing 100191, China

⁴Department of ICT and Natural Sciences, Norwegian University of Science and Technology, 6025 Aalesund, Norway

Corresponding author: Sheng Hong (shenghong@buaa.edu.cn)

This work was supported in part by the National Natural Science Foundation of China under Grant 61572057 and Grant 61773001, in part by the National Key Research and Development Program of China under Grant 2018YFB1004001, in part by the Beijing Natural Science Foundation-Rail Traffic Control Science and Technology Joint Fund under Grant 16L10010, in part by the Beijing Natural Science Foundation under Grant 172023, and in part by the Fundamental Research Funds for the Central Universities under Grant YWF-17-BJ-Y-83.

ABSTRACT Accurate prediction of remaining useful life (RUL) of lithium-ion battery plays an increasingly crucial role in the intelligent battery health management systems. The advances in deep learning introduce new data-driven approaches to this problem. This paper proposes an integrated deep learning approach for RUL prediction of lithium-ion battery by integrating autoencoder with deep neural network (DNN). First, we present a multi-dimensional feature extraction method with autoencoder model to represent battery health degradation. Then, the RUL prediction model-based DNN is trained for multi-battery remaining cycle life estimation. The proposed approach is applied to the real data set of lithium-ion battery cycle life from NASA, and the experiment results show that the proposed approach can improve the accuracy of RUL prediction.

INDEX TERMS Lithium-ion battery, remaining useful life, RUL prediction model, deep learning, deep neural network.

I. INTRODUCTION

In the context of modern industry booming, lithium-ion battery technology has been widely used in the vehicle, household equipment, communications, aerospace and other fields. Compared with traditional batteries, lithium-ion battery has many advantages including high output voltage, high energy density, low self-discharge, long cycle life, high reliability, etc. [1]–[3]. And these advantages have contributed to wider applications of lithium-ion battery in more area. The new generation of TOYOTA Prius, Chevrolet Volt, Nissan Leaf and BYD E6 all work with lithium-ion batteries. Especially for space applications, the lithium-ion battery has become the third generation of satellite energy storage battery for nickel-metal hydride battery and nickel-cadmium battery. Some of the projects have been taken into practical production and application. Lithium-ion batteries are widely used as energy such as NASA's Spirit and Opportunity Mars probe, Phoenix Mars Lander, ESA's Mars Express, ROSETTI A platform and Japanese Falcon bird asteroids [4]. At the same time, the safety and reliability of lithium-ion battery have

always been a very important issue in their applications [5]. Battery malfunction may lead to the performance degradation or malfunction of powered equipment or systems, which will increase the cost. Especially if lithium-ion batteries for electric vehicles are mismanaged, it will cause fire and explosion. In 1999, the US space test Air Force Research Laboratory failed due to an abnormal battery internal impedance. In 2013, several Boeing 787 caught fire as a result of a lithium-ion battery failure and caused all airliners to be grounded indefinitely [6], [7]. As a key power source for a variety of industrial systems, lithium-ion battery defects often lead to fatal system failures [8]. And the National Aeronautics and Space Administration (NASA) launched the Mars probe, the battery was over-charge as NASA ignores its status and rotated solar panels to the direction towards the sun, which resulted in over temperature of the battery. Finally, the lack of power supply led to the loss of the detector [9].

Therefore, accurate prediction of Remaining Useful Life (RUL) of lithium-ion battery plays an increasingly crucial role in lithium-ion battery state estimation and

health management [10]. The typical method of lithium-ion battery RUL prediction is usually divided into two categories: model-based [11] and data driven approach [12]–[18]. The comprehensive internal state data, however, is typically difficult to detect and collect for battery degradation modeling due to the highly complex chemical reactions inside lithium-ion battery. The state of lithium-ion battery is highly vulnerable in addition to working temperature, circuit, load and other environmental factors, therefore it is difficult to establish an accurate prediction model for lithium-ion battery degradation. The data-driven method has recently drawn significant attention in lithium-ion battery RUL prediction research area. Yet most data-driven methods are focused on making short-time prediction for a same battery based on the historical data of the battery, few existing methods can realize multi-battery prediction by using data from multi-battery. The advances in Artificial Intelligence (AI) and Deep Learning introduce new data-driven approaches to this problem. Especially Deep Neural Network (DNN) is suitable for high complex non-linear fitting by training multi-layer artificial neural networks, and can achieve better accuracy for complex prediction problems such as multi-battery RUL estimation.

In this paper, we have consulted a large number of literature [19]–[22]. And to address these issues, this paper proposes an integrated deep learning approach, ADNN, for RUL prediction of multiple lithium-ion battery by integrating autoencoder with DNN. A 21-dimensional feature extraction method with autoencoder model is proposed to represent battery health degradation. And the DNN based RUL prediction model is trained for multi-battery remaining cycle life estimation. The proposed approach is applied to the real dataset of lithium-ion battery cycle life from NASA, and the experimental results show the effectiveness and superiority of the proposed approach. The rest part of the paper is organized as follows. Section 2 investigates related work. Section 3 presents the integrated deep learning approach framework for lithium-ion battery RUL prediction, including the process of feature extraction, feature fusion, data normalization, model training and result evaluation. The experimental implementation and results discussion are described in Section 4. Section 5 concludes the work.

II. RELATED WORK

A. LITHIUM-ION BATTERY RUL PREDICTION METHODS

1) MODEL-DRIVEN METHOD

Xu and Chen [14] predicted the RUL of lithium-ion batteries by establishing a state-space model. The updating of parameters and states in this model is achieved through the combination of Expectation Maximization (EM) and Extended Kalman Filter (EKF) algorithms. Hu *et al.* [5] proposed a moving horizon estimation (MHE) framework for condition monitoring in advanced battery management systems using a reduced-form electrochemical model.

2) DATA-DRIVEN METHOD

Hu *et al.* [23] proposed a data-driven forecasting model for by using a combination of sample entropy and sparse Bayesian predictive modeling. Song *et al.* [12] provided a hybrid method of IND-AR model and PF (Particle Filter) algorithm to predict the remaining life of lithium-ion battery cycles and achieved good results. Liu *et al.* [15] used an Adaptive Recurrent Neural Network (ARNN) algorithm for state prediction of dynamic system. The ARNN algorithm took the Recurrent Levenberg-Marquardt (RLM) method to make several rectifications in the weights of RNN architecture and gained satisfied results in the lithium-ion battery RUL estimation. Wu *et al.* [16] analyzed the battery terminal voltage curves at different cycles during charging, and proposed an online method using feed forward neural network (FFNN) and importance sampling (IS) to estimate lithium-ion battery RUL. Patil *et al.* [13] proposed a real-time RUL estimation method for lithium-ion battery based on the classification and regression properties of machine learning techniques based on Support Vector Machine (SVM). By analyzing the different working conditions of lithium-ion battery cycle data, and extracted the key features from the voltage and temperature curve, and then used these features to train the model, so as to achieve the purpose of lithium-ion battery RUL forecast. Cheng *et al.* [17] proposed a method based on functional principal component analysis (FPCA) and Bayesian lithium battery RUL prediction. FPCA was used to construct a lithium-ion battery degradation model and the Bayesian model was used to update the model parameters Realize the lithium-ion battery RUL forecast. Hong *et al.* [24] proposed a novel performance degradation assessment method for bearing based on ensemble empirical mode decomposition (EEMD), and Gaussian mixture model (GMM). Saha *et al.* [25] and Zhou *et al.* [26] uses the internal parameters of the battery to build a Relevance Vector Machine (RVM) model and uses Particle filter (PF) particle filter algorithm to determine the adaptive parameters of the RVM model to predict the decline of the lithium battery. However, the long-term prediction ability of the RVM algorithm is poor, so it is difficult to obtain a satisfactory RUL estimation result by directly using the RVM model [26]. In the case of different battery degradations, Lu *et al.* [27] compares the trends of various detection parameters, and extracts 4 geometric features that are sensitive to lithium battery degradation from these figures. They are used as detection parameters to characterize the deterioration of lithium batteries and have achieved good results. Hong *et al.* [28] introduces a preprocessing model of the bearing using wavelet packet-empirical mode decomposition (WP-EMD) for feature extraction.

III. DEEP LEARNING FRAMEWORK FOR LITHIUM-ION BATTERY RUL PREDICTION

Figure 1 shows Lithium-ion battery RUL prediction model framework. Firstly, the characteristics are extracted from the

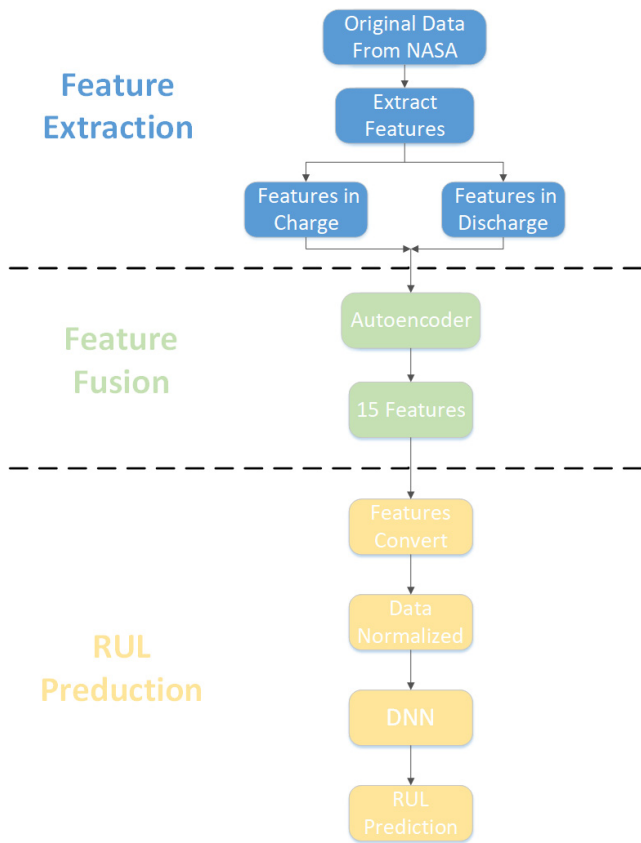


FIGURE 1. Deep learning framework for lithium-ion battery RUL prediction.

original data. Secondly, the feature fusion is performed by the autoencoder model.

Thirdly, the fused features are input to the DNN model to predict the RUL of the lithium-ion battery. Finally, the predicting results are output.

A. FEATURE EXTRACTION

1) ORIGINAL SIGNAL

Via the analysis of the battery charge and discharge process data, it can be found that the charging experiment data includes the battery terminal voltage, the battery output current, the battery temperature, the charger measurement current, the charger measurement voltage and the cycle time vector. Figure 2 shows each charge and discharge cycle. And multiple charging and discharging cycles is to repeat the process of Figure 2.

(a) Charging process: First, a constant current (Constant Current, CC) current lithium-ion battery charge, the voltage was raised to a specific voltage value, and then keep the voltage across the battery is a constant voltage (Constant Voltage, CV) at previous specific value until the charge current drops to a certain value.

(b) Discharging process: Firstly, let the battery discharge at a constant current of a specific current value until the voltage of different lithium-ion batteries drops to a specific voltage value respectively.

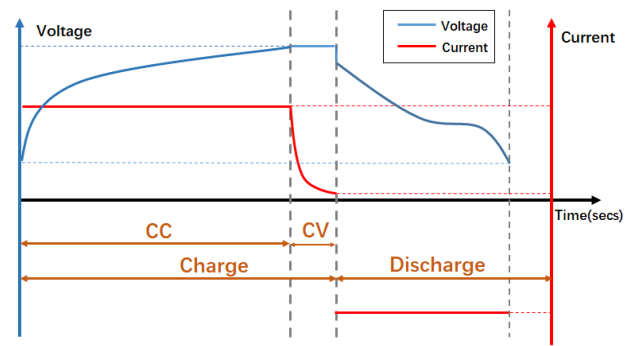


FIGURE 2. Charge and discharge cycle.

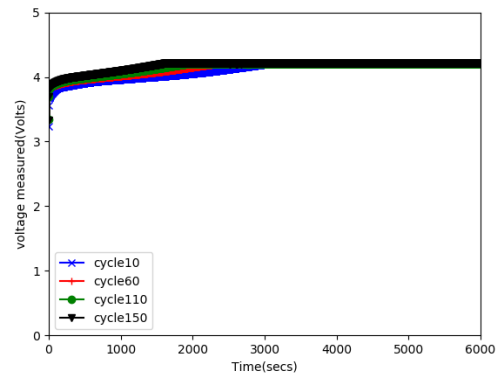


FIGURE 3. Battery terminal voltage and time relationship.

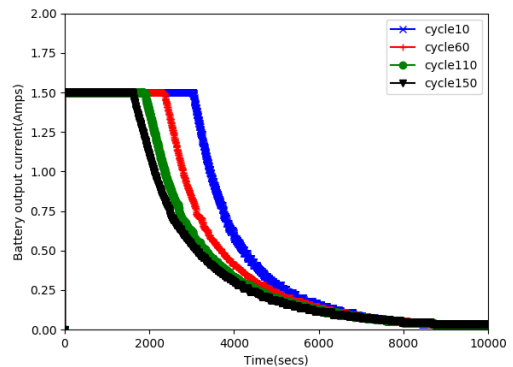


FIGURE 4. Battery output current and time relationship.

Figure 3-7 shows the data of battery terminal voltage, output current, temperature, measured voltage and current over time during multiple charge cycles.

The discharge test data includes: battery terminal voltage, battery output current, battery temperature, load measurement current, voltage measured under load, cycle time vector, battery capacity (Ahr)

During the multiple discharge process, the battery terminal voltage, output current, temperature, voltage measurement, the relationship between time and measuring current changes in data as shown in Figure 8-12.

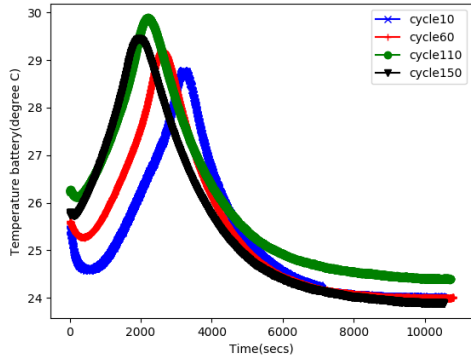


FIGURE 5. Battery temperature and time relationship.

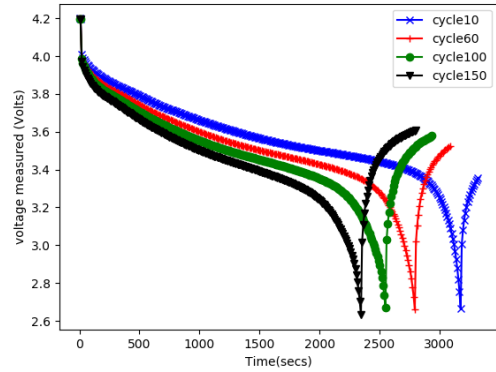


FIGURE 8. voltage measured and time relationship.

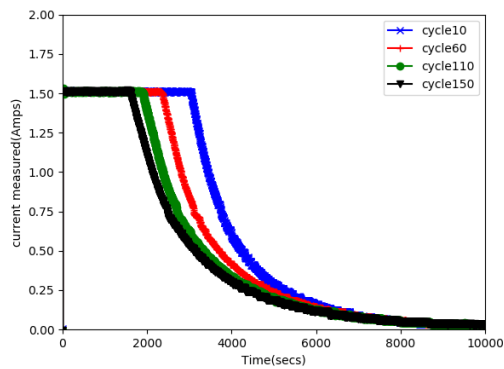


FIGURE 6. Current measured and time relationship.

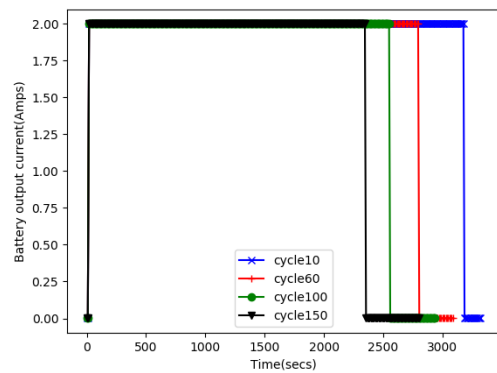


FIGURE 9. Battery output current and time relationship.

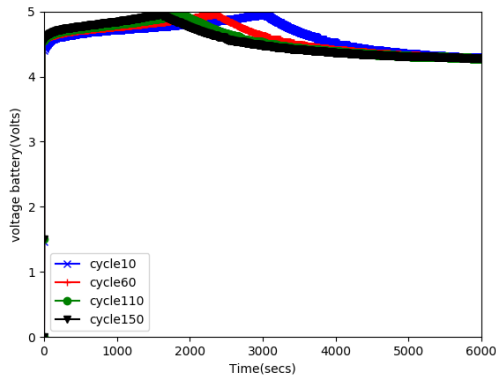


FIGURE 7. Voltage measured and time relationship.

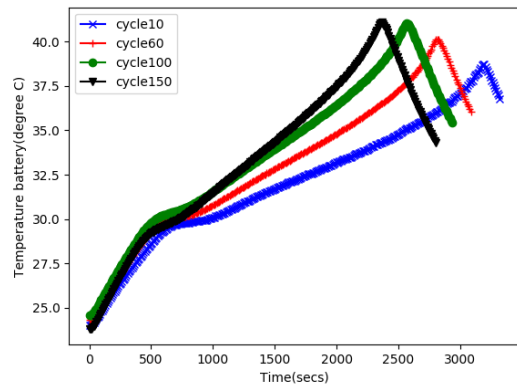


FIGURE 10. Battery temperature and time relationship.

2) EXTRACT FEATURES

Due to the impact of battery life, the sample collected in a battery charge and discharge process is not the same size, and some only 800 sample points, while others have 5000 sample points. Therefore, we can not enter the charge and discharge data directly into the feature fusion model. We need to pre-process the original data, to extract the typical characteristics of each cycle of the battery. There is a positive correlation between informational representation and informational dimension. In theory, the more features extracted from the raw data, the better the prediction.

In order to solve the problem of different sizes of data samples, the intuitive idea is to take the same points at equal intervals for each cycle dimension. And the effect achieved in this way is not satisfying. At the same time of taking the points, it is highly possible to discard the information of some key points in each dimension. Therefore, reliable battery parameters must be determined. These parameters characterize the degradation and actual performance of lithium-ion batteries well, and are still highly reliable and accurate under different cell aging conditions. Meanwhile, the curves for

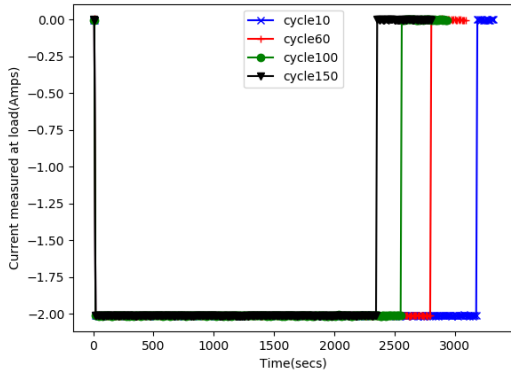


FIGURE 11. Current measured at load and time relationship.

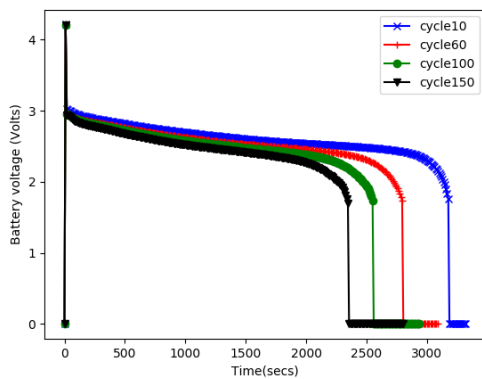


FIGURE 12. Battery voltage and time relationship.

each test parameter of Lithium-ion Battery have obvious geometric characteristics that are very sensitive to the battery's decay [27]. Thus, for each dimension in each charge and discharge cycle, we can extract typical geometric feature information from these dimensions and use these geometric features to characterize the current state of the lithium-ion battery.

In a charging process, the battery terminal voltage extraction features are as in (1).

$$(t_{min\{i\}}, v_i), \quad s.t. v_i \geq 4.2V \quad i = 1, 2, 3 \dots n \quad (1)$$

In the formula, $t_{min\{i\}}$ represents the time when the battery terminal voltage reaches the maximum value first, and v_i represents the value of the output voltage of the battery terminal first reaching the maximum. n is the sample size

Battery output current extraction features are as in (2):

$$(t_{min\{i\}}, A_i), \quad s.t. A_i \leq 1.5V \quad i = 1, 2, 3 \dots n \quad (2)$$

In the formula, $t_{min\{i\}}$ represents the time when the output current of the battery is started to drop, and A_i represents the current value of the battery terminal current starting to drop. n is the sample size.

Battery temperature extraction features are as in (3):

$$(t_{bcT}, T_{bc}) = \{(t_i, T_i)|max(T_i)\} \quad i = 1, 2, 3 \dots n \quad (3)$$

In the formula, t_{bcT} represents the time when the battery temperature reaches the maximum value, T_{bc} represents the highest temperature value. n is the sample size.

Battery measured current extraction features are as in (4):

$$(t_{min\{i\}}, A_i), \quad s.t. A_i \leq 1.5V \quad i = 1, 2, 3 \dots n \quad (4)$$

In the formula, $t_{min\{i\}}$ represents the time when the extracted battery charging current starts to drop. A_i represents the current value when the measured current starts to drop. n is the sample size.

Battery measured voltage extraction features are as in (5):

$$(t_{mcv}, v_{bc}) = \{(t_i, v_i)|max(v_i)\} \quad i = 1, 2, 3 \dots n \quad (5)$$

In the formula, t_{mcv} represents the time when the battery measured voltage reaches the maximum value, v_{bc} represents the highest measured voltage value. n is the sample size

In a discharging process, the battery terminal voltage features are as in (6):

$$(t_{bdv}, v_{bd}) = \{(t_i, v_i)|max(v_i)\} \quad i = 1, 2, 3 \dots n \quad (6)$$

In the formula, t_{bdv} represents the time when the battery terminal voltage reaches the minimum value, v_{bd} represents the minimum voltage value. n is the sample size.

Battery output current extraction features are as in (7):

$$(t_{min\{i\}}, A_i), \quad s.t. A_i > -2A \quad i = 1, 2, 3 \dots n \quad (7)$$

In the formula, $t_{min\{i\}}$ represents the time when the battery output current starts to rise, and A_i represents the current value when the battery output current starts to rise. n is the sample size.

Battery temperature extraction features are as in (8):

$$(t_{bcT}, T_{dc}) = \{(t_i, T_i)|max(T_i)\} \quad i = 1, 2, 3 \dots n \quad (8)$$

In the formula, t_{bcT} represents the time when the battery temperature reaches the maximum value. T_{dc} represents the highest temperature value. n is the sample size.

Load measurement current extraction features are as in (9):

$$(t_{min\{i\}}, A_i), \quad s.t. A_i > -2A \quad i = 1, 2, 3 \dots n \quad (9)$$

In the formula, $t_{min\{i\}}$ represents the time when the load measurement current starts to rise, and A_i represents the current value when the load measurement current starts to rise. n is the sample size.

The formula for extracting the load voltage is:

$$(t_{bcT}, v_{bc}) = \{(t_i, v_i)|min(v_i) \text{ s.t. } v_i \neq 0\} \quad i = 1, 2, 3 \dots n \quad (10)$$

Battery capacitor C directly extracted, when the unit is Ah.

B. FEATURE FUSION

In general, there is a positive correlation between the information characterization and the information dimension. The more information dimensions, the more information representation capability. However, as the number of extracted

features increases, the number of highly correlated features also increases, which often leads to model information redundancy and computational inefficiency. It is necessary to reduce the feature dimension to improve the efficiency of the model. Typical dimensionality reduction methods include principal component analysis (PCA) [29], independent component analysis (ICA) [29], and autoencoder [30]. PCA requires data to be subjected to the Gaussian distribution. Without prior knowledge of the case, it is not suitable for ICA, we cannot determine the distribution of data. Therefore autoencoder will be a good choice.

There are many time-domain features and the combination of different time-domain features is more complex. It is difficult to choose the time-domain features that are suitable for the battery's remaining cycle life prediction. But depth autoencoder network can achieve the fusion of time-domain data. In the model training phase, the input of the network is the time-domain feature vector of the training set, and the output is also the training set of the time-domain feature vector. After training the autoencoder network, we can carry out the feature fusion.

The autoencoder neural network is an unsupervised algorithm that has a completely symmetrical network structure [30]–[32]. It attempts to learn a constant function that the result outputted is close to the target given by input data [33]. In this case, when the output is close to the input, we can use the hidden neurons to express the input, which is shown in Figure 13:

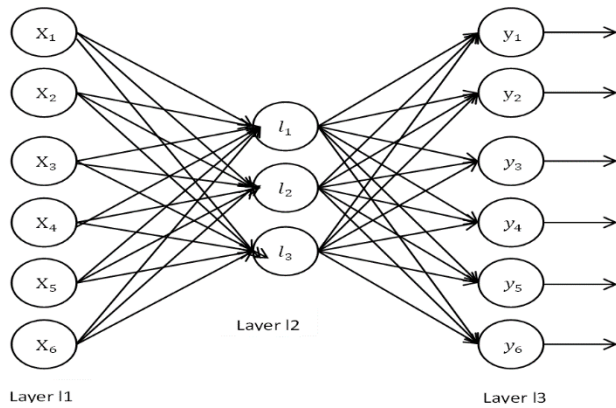


FIGURE 13. Autoencoder model.

Set $\{x^1, x^2, x^3, x^4, x^5, x^6\}$ as input data of the neural network, and the 3-dimensional data is operated in the encoder as there are 3 units set in layer I2. In layer I3 the data will be sent to the decoder. Finally, 6-dimensional output $\{y^1, y^2, y^3, y^4, y^5, y^6\}$ will be generated from units in I3. We train the encoder and decoder so that y^i equals x^i . In this way, we can use $\{l^1, l^2, l^3\}$ to represent $\{x^1, x^2, x^3, x^4, x^5, x^6\}$.

The original feature set encoding process in this article from the input layer to the hidden layer is as in (11):

$$h_i = g\theta_1(x_i) = \sigma(w_1 + x_i + b_1) \quad i = 1, 2 \dots m \quad (11)$$

h_i is a 15-dimensional fusion feature set, x^1 is a 21-dimensional original feature set, w_1 is a weight set, and b_1 is a fixed parameter. m is the number of samples.

From the hidden layer to the output layer decoding process is as in (12):

$$x'_i = g\theta_2(x_i) = \sigma(w_2 h_i + b_2) \quad i = 1, 2, 3 \dots \quad (12)$$

x'_i is a decoded 21-dimensional feature set, w_2 is a set of weights, and b_2 is a fixed parameter.

The reconstruction error loss function for dataset x is as in (13):

$$J_E(W, b) = \frac{1}{m} \sum_{i=1}^m \frac{\|x'_i - x_i\|^2}{2} X_i \quad (13)$$

m is the number of samples, and the sample set minimizes the reconstruction error loss function.

After the training, x' can be treated as another expression of x .

C. DATA CONVERT

After the previous step, i -th charge and discharge data is compressed into a 15-dimensional feature x_i that are input into the RUL prediction model. However, to train the prediction model, it is also necessary to get y_i corresponding to x_i , that is, unsupervised data trained by autoencoder need to be converted to supervised data. The specific process is as follows:

Firstly, we calculate the total number of battery charge and discharge cycles as the total Lithium-ion Battery cycle life n .

Secondly, the i th charge and discharge cycle ($0 < i < n$) RUL y_i is calculated by (14):

$$y_i = n + 1 - i \quad (14)$$

Finally, x_i and y_i are combined to get the supervised data (x_i, y_i) .

D. DATA NORMALIZED

In order to eliminate the negative effects caused by different ranges of values, the range of all extracted eigenvalues is transformed to $[0, 1]$ by the minimum-maximum normalization method [34]. In addition, the feature is transformed into the same interval, which facilitates the overall training of the depth model.

The minimum and maximum normalization method conversion formula is as in (15):

$$X^* = \frac{x - x_{min}}{x_{max} - x_{min}} \quad (15)$$

x_{max} is the maximum value of the sample data and x_{min} is the minimum value of the sample data.

E. TRAIN THE DNN MODEL

The model used for lithium-ion RUL prediction is deep neural networks, which are supervised learning models. In the model training step, the training set needs input and corresponding output. Deep neural network can improve the computation

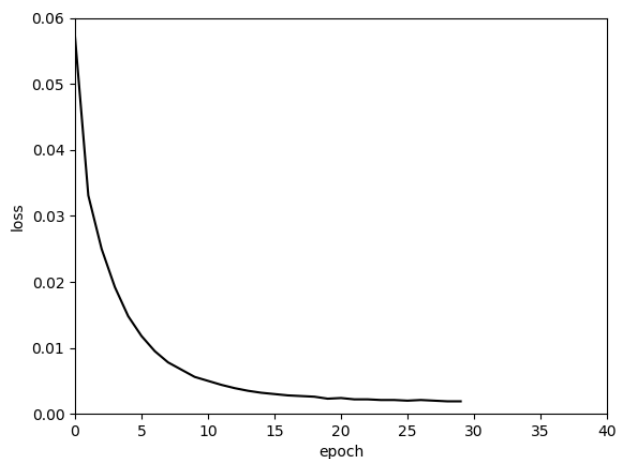


FIGURE 14. Relationship between training lot and loss function.

ability of the training model. As each hidden layer can be a layer of the output of non-linear transformation, the deep neural network has more expressive capability than a shallow one. In the deep neural network model, each hidden layer as well as output layer should use non-linear activation function. The deep neural networks need to randomly initialize the weight of the depth network before using gradient descent method. Vanishing gradient problem often occurs in deep neural networks model training, because inappropriate excessive number of layers could lead to rapid residual fall, resulting in slow updating especially at the earliest layers. Therefore, the configuration of the number of hidden layers is among the most important elements that influence the efficiency of the training model.

The deep neural networks model consists of four fully connected layers, the number of neurons in each layer is: 10, 7, 4, 1. The ReLu function is the activation function of the intermediate hidden layer and the sigmoid function is the activation function of the output layer.

Each round of loss function changes throughout the training process are shown below:

F. RUL PREDICTION AND EVALUATION

By using a trained DNN model, lithium-ion battery RUL can be predicted. In order to evaluate the performance of deep neural network models, the prediction results need to be compared with Bayesian regression [35], support vector machine (SVM) [36] and linear regression [37]. Root Mean Square Error (RMSE) is used to assess prediction accuracy and to compare the performance of different prediction models.

RMSE formula is as in (16):

$$x_{RMSE} = \sqrt{\frac{\sum_{i=1}^n (x_{predict.i} - x_{mod el.i})^2}{n}} \quad (16)$$

n is the size of the test set, $x_{predict.i}$ is the predicted value of the sample i , and $x_{mod el.i}$ is the true value of the sample i .

IV. EXPERIMENTS

A. DATA DESCRIPTION

we adopt the lithium-ion battery batteries data set from NASA AMES Center [38], [39]. The battery data set is from the NASA PCoE.

In this paper, we use the three lithium-ion battery data of B5, B6 and B7 in this data set to accelerate in three different operation modes of charging, discharging and electrochemical impedance measurement under 25 degrees Celsius Degradation of the experiment, and record the observed data. The specific steps are as follows:

(1) Charging process: First, a constant current (Constant Current, CC) 1.5A current lithium-ion battery charge, the voltage was raised to 4.2V, and then keep the voltage across the battery is a constant voltage (Constant Voltage, CV) at 4.2V until the charge current drops to 20mA.

(2) Discharge process: Firstly, let the battery discharge at a constant current of 2A until the voltage of three lithium-ion batteries B5, B6 and B7 drops to 2.7V, 2.5V and 2.2V respectively.

Experiments need to constantly repeat the battery above three operations to speed up the battery recession process. Impedance measurements provide us with insight into how the battery's internal parameters change as the battery decays. When battery capacity decays to 70%, battery life ends and the experiment ends. It should be noted that the impedance measurement needs to be carried out between the recharging and discharging process so as to collect the battery parameter data better.

B. FEATURE EXTRACTION

The battery characteristics of # 5, # 6, and # 7 were extracted as described in Section 3.1, and the data of # 5 and # 6 batteries were used as the training set and the data of # 7 battery as the test set.

C. FEATURE FUSION BY AUTOENCODER

The features extracted from # 5 and # 6 were input into the autoencoder model, and the features were compressed into 15 dimensions by training the model. The autoencoder model consisted of three layers, the ReLu function was the activation function of the hidden layer, and the sigmoid function was the activation function of the output layer.

D. DATA CONVERT AND NORMALIZED

Because there are 168 charge and discharge cycles on the #5 battery, the RUL value corresponding to the i th charge and discharge cycle is $169-i$, so that the supervised data of the #5 battery can be obtained. In the same way, there is supervised data for #6 Battery

Different features have different values ranges, which will have a negative impact on the training of the model. In order to eliminate this effect, we transformed the range of the compressed features to $[0, 1]$ using the minimum-maximum normalization method.

E. TRAIN THE DNN MODEL

DNN's parameters were trained using normalized training data. The input of the DNN model was a set of features, with a total of 15 features and output is the RUL of lithium-ion battery. The loss function was mean squared error, and the optimization algorithm adopts stochastic gradient descent algorithm. After trained, the DNN model could be used to predict the RUL of lithium-ion battery. Input the feature set, a total of 15 features, to the DNN model, and the model output was the RUL of lithium-ion battery.

F. RUL PREDICTION AND EVALUATION

The data of the # 7 battery were used to test the model performance, and the predicted results were compared with the Bayesian regression model, the SVM model and the linear regression model. RMSE was used to evaluate the predictive effects of different models.

G. RESULTS AND DISCUSSION

The experiments were repeated many times and initially got special good results in some cases. Now that more supplementary experiments have been done, the experimental results have stabilized. Figure 15 shows the results of a # 7 battery prediction with Autoencoder and DNN models (ADNN). The horizontal axis represents the 21-dimensional feature set extracted from each charge and discharge cycle, and the vertical axis represents the normalized values of remaining cycle times for lithium-ion battery corresponding to the secondary charge and discharge process. The red line shows the true values (normalized remaining cycle times) and the black dotted line shows the predicted values. The RUL prediction curve is in good agreement with the observed data. RMSE is 11.80%, and the accuracy rate is 88.20%.

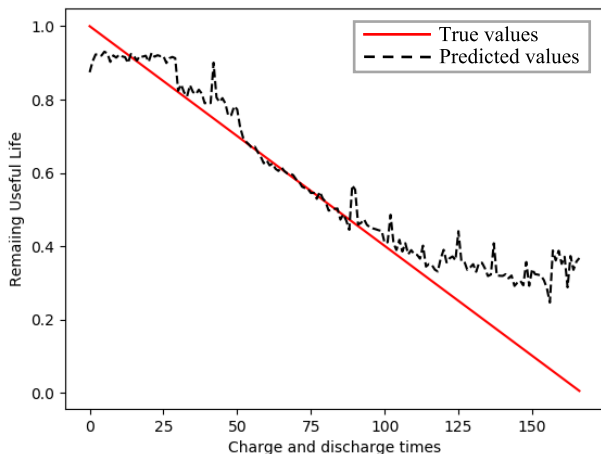


FIGURE 15. The prediction results of ADNN.

Figure 16 shows the results of a Bayesian regression model for predicting a # 7 cell. The red line shows the true value

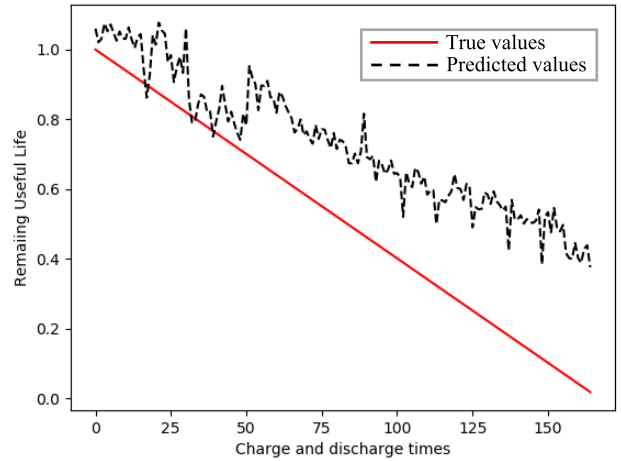


FIGURE 16. The prediction results of Bayesian Regression.

and the black dotted line shows the predicted value. RMSE is 24.72%, the accuracy rate is 75,28%.

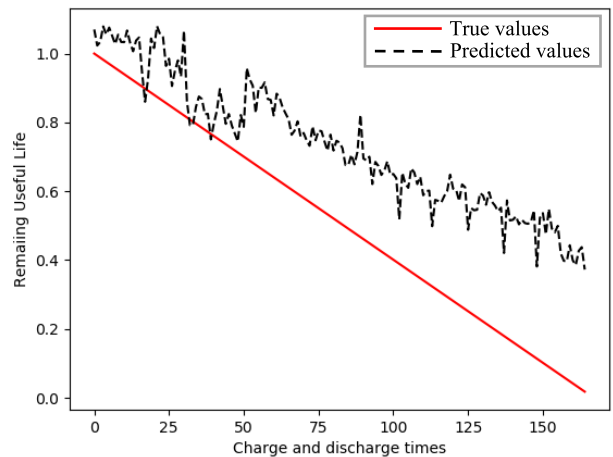


FIGURE 17. The prediction results of Linear Regression.

Figure 17 shows the results of a #7 battery prediction using a linear regression model. The red line shows the true value and the black dotted line shows the predicted value. RMSE is 24.99% with an accuracy of 75.01%.

Figure 18 shows the results of a #7 battery prediction using the SVM model. The red line shows the true value and the black dotted line shows the predicted value. RMSE is 18.23%, the accuracy rate is 81.77%.

As shown in Table 1, the comparison results show that ADNN can achieve better accuracy for lithium-ion battery RUL prediction.

Figure 19 shows the predicted results from the 20 charge and discharge cycles of #7 battery when using the ADNN model. The red line shows the true value and the black dotted line shows the predicted value. RMSE is 12.41%, and accuracy is 87.59%.

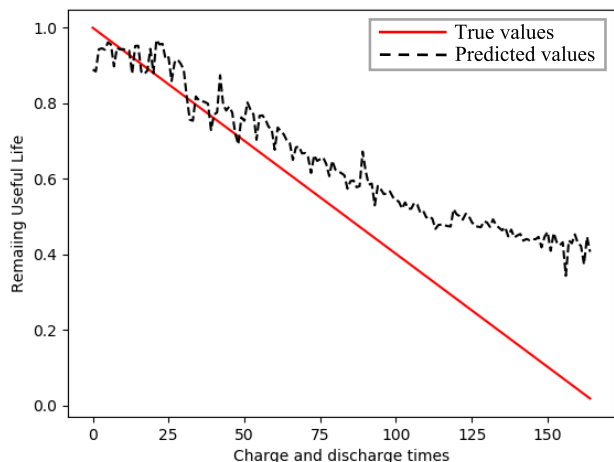


FIGURE 18. The prediction results of SVM.

TABLE 1. Comparison of experimental results.

method	RMSE	Accuracy
ADNN	6.66%	93.34%
Bayesian regression	11.92%	89.08%
Linear regression	12%	88%
SVM	10.66%	89.34%

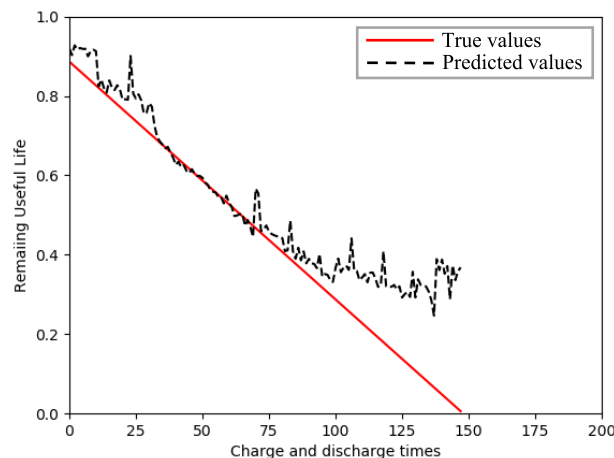


FIGURE 19. The prediction results of ADNN after 20 cycles.

Figure 20 shows the predicted results from the 20 charge and discharge cycles of #7 battery when using the BVAR model. The red line shows the true value and the black dotted line shows the predicted value. RMSE is 26.09%, and accuracy is 73.91%.

Figure 21 shows the predicted results from the 20 charge and discharge cycles of #7 battery when using the linear

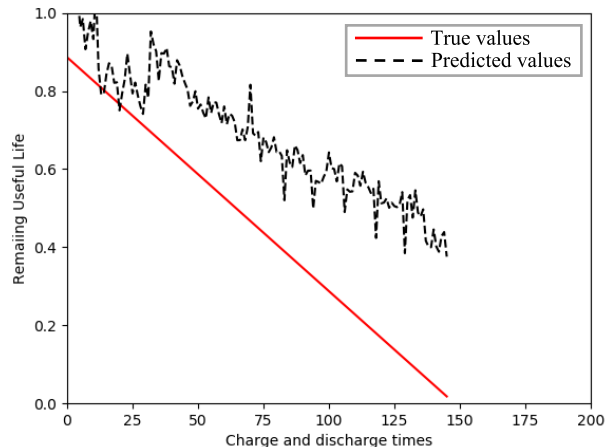


FIGURE 20. The prediction results of Bayesian Regression after 20 cycles.

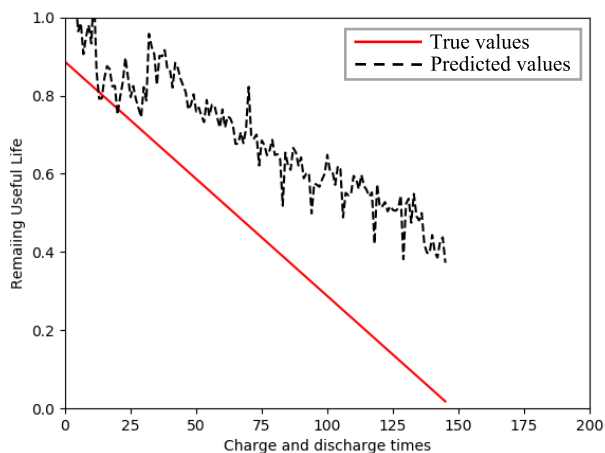


FIGURE 21. The prediction results of Linear Regression after 20 cycles.

regression model. The red line shows the true value and the black dotted line shows the predicted value. RMSE is 26.38%, and accuracy is 73.64%.

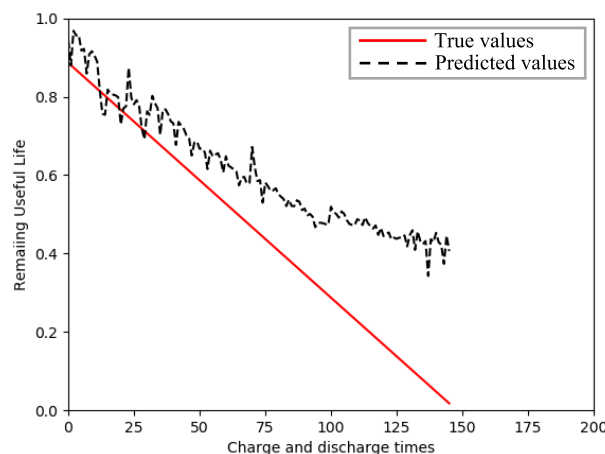


FIGURE 22. The prediction results of SVM after 20 cycles.

Figure 22 shows the predicted results from the 20 charge and discharge cycles of #7 battery when using the

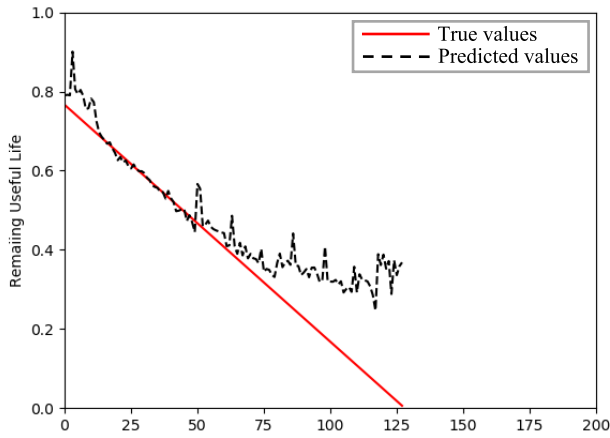


FIGURE 23. The prediction results of ADNN after 40 cycles.

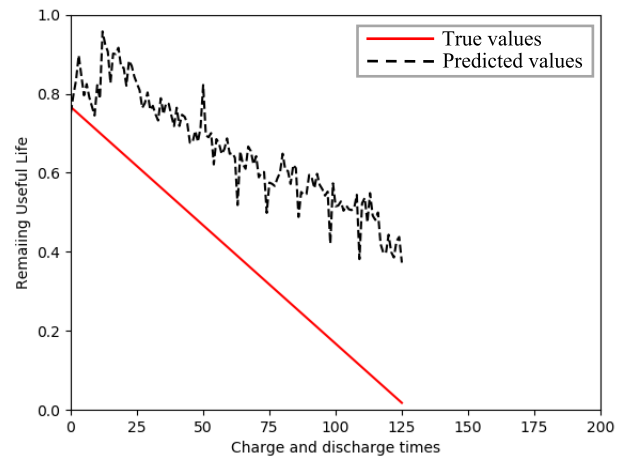


FIGURE 25. The prediction results of Linear Regression after 20 cycles.

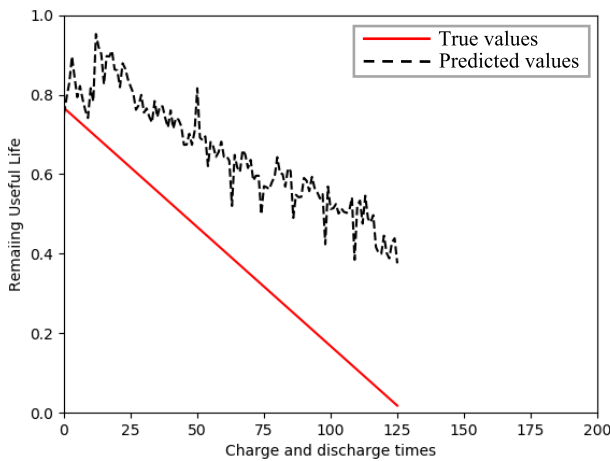


FIGURE 24. The prediction results of Bayesian Regression after 20 cycles.

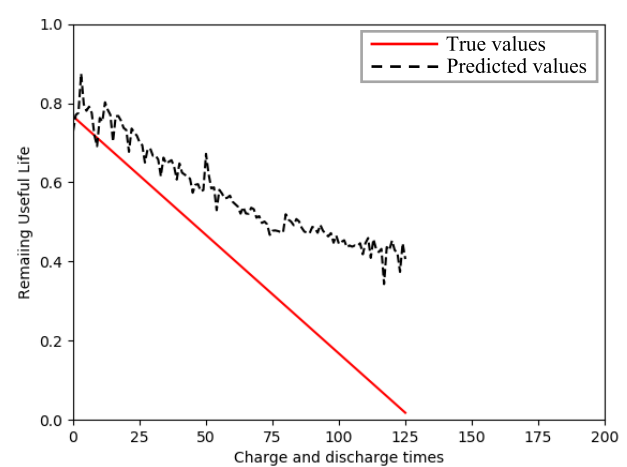


FIGURE 26. The prediction results of SVM after 40 cycles.

SVM model. The red line shows the true value and the black dotted line shows the predicted value. RMSE is 19.31%, and accuracy is 80.69%.

Figure 23 shows the predicted results from the 40 charge and discharge cycles of #7 battery when using the ADNN model. The red line shows the true value and the black dotted line shows the predicted value. RMSE is 13.20%, and accuracy is 86.80%.

Figure 24 shows the predicted results from the 40 charge and discharge cycles of #7 battery when using the BVAR model. The red line shows the true value and the black dotted line shows the predicted value. RMSE is 27.65%, and accuracy is 72.35%.

Figure 25 shows the predicted results from the 40 charge and discharge cycles of #7 battery when using the linear regression model. The red line shows the true value and the black dotted line shows the predicted value. RMSE is 27.94%, and accuracy is 72.06%.

Figure 26 shows the predicted results from the 40 charge and discharge cycles of #7 battery when using the SVM model. The red line shows the true value and the black

dotted line shows the predicted value. RMSE is 20.66%, and accuracy is 79.34% SVM RMSE 20.66%.

From the above experiments, it can be seen that the ADNN algorithm can track the early and mid-term decline of lithium batteries well, but the prediction of the late decline of lithium batteries is poor, which is because that the extracted 21-dimensional features cannot reflect the late changes of lithium batteries.

V. CONCLUSION

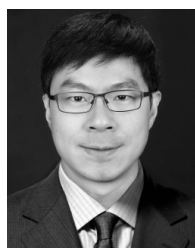
RUL prediction is of great importance to the state estimation and health management of lithium-ion battery. The developments of AI and deep learning areas provide a new promising methods for lithium-ion battery RUL prediction. The main contributions can be summarized as follows: (1) A new 21-dimensional feature extraction method using autoencoder is proposed to characterize battery health degradation; and (2) an autoencoder-DNN integrated deep learning approach, ADNN, is proposed for multiple lithium-ion battery RUL prediction. We applied the proposed approach to the real dataset of lithium-ion battery cycle life from NASA.

The experimental results show the effectiveness and better accuracy of the proposed approach by comparison with the linear regression, Bayesian regression, support vector machines and other shallow models.

In future work we plan to improve the proposed approach for lithium-ion battery RUL prediction in the context of different working conditions.

REFERENCES

- [1] J. Zhang and J. Lee, "A review on prognostics and health monitoring of Li-ion battery," *J. Power Sources*, vol. 196, pp. 6007–6014, Aug. 2011.
- [2] W. He, N. Williard, M. Osterman, and M. Pecht, "Prognostics of lithium-ion batteries based on Dempster–Shafer theory and the Bayesian Monte Carlo method," *J. Power Sources*, vol. 196, no. 23, pp. 10314–10321, 2011.
- [3] X. Hu, C. Zou, C. Zhang, and Y. Li, "Technological developments in batteries: A survey of principal roles, types, and management needs," *IEEE Power Energy Mag.*, vol. 15, no. 5, pp. 20–31, Sep. 2017.
- [4] D. Liu, J. Zhou, and Y. Peng, "Data-driven prognostics and remaining useful life estimation for lithium-ion battery: A review," *Instrumentation*, vol. 1, no. 1, pp. 59–70, 2014.
- [5] X. Hu, D. Cao, and B. Egardt, "Condition monitoring in advanced battery management systems: Moving horizon estimation using a reduced electrochemical model," *IEEE/ASME Trans. Mechatronics*, vol. 23, no. 1, pp. 167–178, Feb. 2018.
- [6] K. Goebel, B. Saha, A. Saxena, J. R. Celaya, and J. P. Christophersen, "Prognostics in battery health management," *IEEE Instrum. Meas. Mag.*, vol. 11, no. 4, pp. 33–40, Aug. 2008.
- [7] N. Williard, W. He, C. Hendricks, and M. Pecht, "Lessons learned from the 787 Dreamliner issue on lithium-ion battery reliability," *Energies*, vol. 6, no. 9, pp. 4682–4695, 2013.
- [8] Y. Xing, E. W. M. Ma, K. L. Tsui, and M. Pecht, "Battery management systems in electric and hybrid vehicles," *Energies*, vol. 4, no. 11, pp. 1840–1857, 2011.
- [9] D. Le and X. Tang, "Lithium-ion battery state of health estimation using Ah-V characterization," in *Proc. Annu. Conf. Prognostics Health Manage. (PHM) Soc.*, Montreal, QC, Canada, vol. 2629, Sep. 2011, pp. 367–373.
- [10] Y. Wang, R. Pan, D. Yang, X. Tang, and Z. Chen, "Remaining useful life prediction of lithium-ion battery based on discrete wavelet transform," *Energy Procedia*, vol. 105, pp. 2053–2058, May 2017.
- [11] A. V. Virkar, "A model for degradation of electrochemical devices based on linear non-equilibrium thermodynamics and its application to lithium ion batteries," *J. Power Sources*, vol. 196, no. 14, pp. 5970–5984, Jul. 2011.
- [12] Y. Song, D. Liu, C. Yang, and Y. Peng, "Data-driven hybrid remaining useful life estimation approach for spacecraft lithium-ion battery," *Microelectron. Rel.*, vol. 75, pp. 142–153, Aug. 2017.
- [13] M. A. Patil et al., "A novel multistage support vector machine based approach for Li ion battery remaining useful life estimation," *Appl. Energy*, vol. 159, pp. 285–297, Dec. 2015.
- [14] X. Xu and N. Chen, "A state-space-based prognostics model for lithium-ion battery degradation," *Rel. Eng. Syst. Saf.*, vol. 159, pp. 47–57, Mar. 2017.
- [15] J. Liu, A. Saxena, K. Goebel, B. Saha, and W. Wang, "An adaptive recurrent neural network for remaining useful life prediction of lithium-ion batteries," in *Proc. Annu. Conf. Prognostics Health Manage. Soc.*, Portland, OR, USA, Oct. 2010.
- [16] J. Wu, C. Zhang, and Z. Chen, "An online method for lithium-ion battery remaining useful life estimation using importance sampling and neural networks," *Appl. Energy*, vol. 173, pp. 134–140, Jul. 2016.
- [17] Y. Cheng, C. Lu, T. Li, and L. Tao, "Residual lifetime prediction for lithium-ion battery based on functional principal component analysis and Bayesian approach," *Energy*, vol. 90, pp. 1983–1993, Oct. 2015.
- [18] S. Hong, Z. Zhou, E. Zio, and W. Wang, "An adaptive method for health trend prediction of rotating bearings," *Digit. Signal Process.*, vol. 35, pp. 117–123, Dec. 2014.
- [19] S. Hong, X. Zhang, J. Zhu, T. Zhao, and B. Wang, "Suppressing failure cascades in interconnected networks: Considering capacity allocation pattern and load redistribution," *Mod. Phys. Lett. B*, vol. 30, no. 5, p. 1650049, 2016.
- [20] S. Hong, C. Lv, T. Zhao, B. Wang, J. Wang, and J. Zhu, "Cascading failure analysis and restoration strategy in an interdependent network," *J. Phys. A, Math. Theor.*, vol. 49, no. 19, p. 195101, 2016.
- [21] S. Hong, H. Yang, T. Zhao, and X. Ma, "Epidemic spreading model of complex dynamical network with the heterogeneity of nodes," *Int. J. Syst. Sci.*, vol. 47, no. 11, pp. 2745–2752, 2016.
- [22] S. Hong, B. Wang, X. Ma, J. Wang, and T. Zhao, "Failure cascade in interdependent network with traffic loads," *J. Phys. A, Math. Theor.*, vol. 48, no. 48, p. 485101, 2015.
- [23] X. Hu, J. Jiang, D. Cao, and B. Egardt, "Battery health prognosis for electric vehicles using sample entropy and sparse Bayesian predictive modeling," *IEEE Trans. Ind. Electron.*, vol. 63, no. 4, pp. 2645–2656, Apr. 2016.
- [24] S. Hong, B. Wang, G. Li, and Q. Hong, "Performance degradation assessment for bearing based on ensemble empirical mode decomposition and Gaussian mixture model," *J. Vib. Acoust.*, vol. 136, no. 6, p. 061006, 2014.
- [25] B. Saha, S. Poll, K. Goebel, and J. Christophersen, "An integrated approach to battery health monitoring using Bayesian regression and state estimation," in *Proc. IEEE Autotestcon*, Sep. 2007, pp. 646–653.
- [26] J. Zhou, S. Wang, L. Ma, S. Yang, Y. Peng, and X. Peng, "Study on the reconfigurable remaining useful life estimation system for satellite lithium-ion battery," *Chin. J. Sci. Instrum.*, vol. 34, no. 9, pp. 2034–2044, 2013.
- [27] C. Lu, L. Tao, and H. Fan, "Li-ion battery capacity estimation: A geometrical approach," *J. Power Sources*, vol. 261, pp. 141–147, Sep. 2014.
- [28] S. Hong, Z. Zhou, E. Zio, and K. Hong, "Condition assessment for the performance degradation of bearing based on a combinatorial feature extraction method," *Digit. Signal Process.*, vol. 27, pp. 159–166, Apr. 2014.
- [29] M. S. Reza and J. Ma, "ICA and PCA integrated feature extraction for classification," in *Proc. IEEE 13th Int. Conf. Signal Process. (ICSP)*, Nov. 2017, pp. 1083–1088.
- [30] Y. Wu, C. DuBois, A. X. Zheng, and M. Ester, "Collaborative denoising auto-encoders for top-N recommender systems," in *Proc. 9th ACM Int. Conf. Web Search Data Mining*, 2016, pp. 153–162.
- [31] Y. Burda, R. Grosse, and R. Salakhutdinov, "Importance weighted autoencoders," *Comput. Sci.*, 2015.
- [32] A. Makhzani et al., "Adversarial autoencoders," *Comput. Sci.*, vol. abs/1511.05644, 2015. [Online]. Available: <http://arxiv.org/abs/1511.05644>
- [33] N. Akhtar, F. Sahfai, and A. Mian, "Repeated constrained sparse coding with partial dictionaries for hyperspectral unmixing," in *Proc. IEEE Winter Conf. Appl. Comput. Vis. (WACV)*, Mar. 2014, pp. 953–960.
- [34] G. K. Mislick and D. A. Nussbaum, *Data Normalization. Cost Estimation: Methods and Tools*. Hoboken, NJ, USA: Wiley, 2015, pp. 78–104.
- [35] L. N. Geppert, K. Ickstadt, A. Munteanu, J. Quedenfeld, and C. Sohler, "Random projections for Bayesian regression," *Statist. Comput.*, vol. 27, no. 1, pp. 79–101, 2017.
- [36] D. Cui and D. Curry, "Prediction in marketing using the support vector machine," *Marketing Sci.*, vol. 24, no. 4, pp. 595–615, 2005.
- [37] R. R. Hocking, "A biometrics invited paper. The analysis and selection of variables in linear regression," *Biometrics*, vol. 32, no. 1, pp. 1–49, 1976.
- [38] B. Saha, K. Goebel, and J. Christophersen, "Comparison of prognostic algorithms for estimating remaining useful life of batteries," *Trans. Inst. Meas. Control*, vol. 31, nos. 3–4, pp. 293–308, 2009.
- [39] B. Saha and K. Goebel, "Battery data set," NASA Ames Prognostics Data Repository, NASA Ames, Moffett Field, CA, USA, Tech. Rep., 2007. [Online]. Available: <http://ti.arc.nasa.gov/project/prognostic-datarepository>



LEI REN (M'17) received the Ph.D. degree in computer science from the Institute of Software, Chinese Academy of Sciences, in 2009. He is currently an Associate Professor and the Deputy Head of the Cloud Manufacturing Research Center, School of Automation Science and Electrical Engineering, Beihang University, and a Senior Research Scientist with the Engineering Research Center of Complex Product Advanced Manufacturing Systems, Ministry of Education, China.

He has published over 50 papers and over 2000 citations according to Google Scholar. He edited a book *Challenges and Opportunity with Big Data* (Springer LNCS). His research interests include big data analytics and applications. He is a member of the ACM, ASME, and SCS. He also served as a TPC Co-Chair for the 19th Monterey Workshop on Big Data and the 5th International Conference on Enterprise Systems. He served as an Associate Editor of *SIMULATION: Transactions of the Society for Modeling and Simulation International*, and reviewers for journals, such as the IEEE TII, TSMC, and ACM TCC.



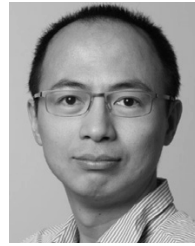
LI ZHAO is currently pursuing the Ph.D. degree with the School of Automation Science and Electrical Engineering, Beihang University. His research interests include deep learning, data-driven methods, and remaining useful life prediction of lithium-ion battery.



SHENG HONG received the master's and the Ph.D. degrees in communication and information system from Beihang University in 2005 and 2009, respectively. He is currently an Associate Professor with the School of Cyber Science and Technology, Beihang University. His recent interests include signal processing, information system modeling, prognostics, and health management.



SHIQIANG ZHAO is currently pursuing the Ph.D. degree with the School of Automation Science and Electrical Engineering, Beihang University. His research interests include deep learning and data-driven methods.



HAO WANG is currently an Associate Professor and the Head of the Big Data Laboratory, Department of ICT and Natural Sciences, Norwegian University of Science and Technology, Norway. He was a Researcher with IBM Canada, McMaster, and St. Francis Xavier University, before he moved to Norway. His research interests include big data analytics and industrial Internet of Things, high-performance computing, safety-critical systems, and communication security. He has authored over 60 papers in the *IEEE TVT*, *GlobalCom 2016*, *Sensors*, the *IEEE Design & Test*, *Computer Communications*. He is a member of the IEEE IES Technical Committee on Industrial Informatics. He served as a TPC Co-Chair for the *IEEE DataCom 2015*, the *IEEE CIT 2017*, and *ES 2017*, and a reviewer for journals, such as the *IEEE TKDE*, *TBD*, *TETC*, *T-IFS*, and the *ACM TOMM*. His webpage is www.haowang.no.



LIN ZHANG is a Full Professor with Beihang University. He received the B.S. degree in 1986 from the Department of Computer and System Science at Nankai University, China, the M.S. degree and the Ph.D. degree in 1989 and 1992 from the Department of Automation at Tsinghua University, China. From 2002 to 2005 he worked at the US Naval Postgraduate School as a senior research associate of the US National Research Council. His research interests include complex systems modeling and simulation, data science, and model engineering for simulation. He serves as the Past President of the Society for Modeling & Simulation International (SCS), a vice president of the Chinese Simulation Federation (CSF), Fellow of ASIASIM, a board member of CAAI, a senior member of IEEE, a member of IEEE TC on Industrial Informatics, the chief scientist of key projects of China High-Tech R&D Program (863), and associate Editor-in-Chief and associate editors of 6 peer-reviewed international journals. He authored and co-authored 200 papers, 10 books and chapters. He received the National Award for Excellent Science and Technology Books in 1999, the 863 Outstanding Individual Award in 2001, the National Excellent Scientific and Technological Workers Awards in 2014.

• • •